JOURNAL OF SOLID STATE CHEMISTRY 1, 332–338 (1970)

Preparation and Properties of Molybdenum Fluoro-Bronzes†

J. W. PIERCE, H. L. McKINZIE, M. VLASSE, AND A. WOLD

Department of Chemistry and Division of Engineering, Brown University, Providence, Rhode Island 02912

Received October 9, 1969

Partial substitution of fluorine for oxygen in MoO_3 was achieved by reacting Mo and MoO_3 under 2-kb pressure in the presence of concentrated HF. Two new bronze-like phases having the compositions $Mo_4O_{11.2}F_{0.8}$ (orthorhombic) and $MoO_{2.4}F_{0.6}$ (cubic) were prepared. X-ray diffraction data show the structure of the cubic phase to be similar to that of ReO_3 while the orthorhombic phase has a structure similar to that of $Mo_4O_{10}(OH)_2$. Single crystal resistivity data show the cubic phase to be metallic and the orthorhombic phase to be a sermiconductor.

Introduction

The structural chemistry of the molybdenum and tungsten oxide systems has been the subject of extensive studies and this work is reviewed in papers by Hägg, Magnéli, and Kihlborg (*1*) and (*2*). The structures of MoO_2 and MoO_3, as well as those of a number of intermediate oxides, have been established (*3*)–(*5*) and in addition Wilhelmi (*6*) has recently determined the structure of $Mo_4O_{10}(OH)_2$ and related it to those of MoO_3 and $Mo_{18}O_{52}$.

For these structures the basic building unit is a distorted MoO_6 octahedron. However, the degree of distortion may be large enough to significantly alter the coordination number of the molybdenum atoms. In the MoO_3 structure the molybdenum atoms have a strong tendency towards four-fold coordination, in $Mo_4O_{10}(OH)_2$ the Mo atoms have five oxygen neighbors, and in Mo_4O_{11} the coordination number of Mo approaches six.

It was first suggested by Magnéli (*7*) that an increase in the amount of reduced molybdenum present in the compound is accompanied by an increase in the coordination number of the Mo atoms. In addition to the synthesis of $Mo_4O_{10}(OH)_2$ by Wilhelmi (*6*), LaValle et al. (*8*) have indicated that the ranges of x in the system $MoO_{3-x}F_x$ has not been well established.

Stoichiometric ReO_3 (*9*) has been reported to be metallic. One-electron molecular-orbital energy diagrams have been proposed by Goodenough (*10*) that can explain the electrical properties of these materials on the basis of strong covalent mixing between the cation t_{2g} and oxygen p_π orbitals. This mixing allows sufficient interaction between cations on opposite sides of an anion so that the conditions for localized d electrons break down. The resulting d-like collective-electron orbitals, which are antibonding with respect to the anion array, are designated π^* orbitals. Metallic behavior occurs where these bands exist and are partially occupied. It is interesting to inquire how substitution of oxygen by fluorine influences the formation of these bands.

The work of Wilhelmi (*6*) indicated the possible existence of additional molybdenum oxyfluoride phases related to the more distorted MoO_3 structure. It was anticipated that if such compounds existed they would show semiconducting behavior.

Experimental

Preparation of Materials

The hydrothermal syntheses were performed with commercially available equipment† arranged so that the pressure could be monitored during the course of the reaction. Iron-constantan thermocouples were attached to the outside of the pressure vessel and measured the temperature to within ±2°C. The reactions were carried out at 500°C and 2-kb pressure unless otherwise stated. A quench to room temperature and atmospheric pressure was

† This research has been supported by A.R.P.A. and N.S.F. Grant No. GP-10231.

† A model HR-2C-2 hydrothermal bench was used in conjunction with modified LRA-150 Rene steel pressure vessels. This equipment was obtained through Tem-Pres Research Inc., State College, Pa.

accomplished by submerging the pressure vessel in water.

Mixtures of reagent grade MoO_3 and powdered molybdenum metal were weighed out in the desired mole ratio and placed in containers formed by sealing one end of a 10-cm length of 5-mm i.d. gold tubing. The desired amount of reagent grade 48% hydrofluoric acid was added dropwise to the reaction mixture. In most cases the mole ratio of HF to molybdenum in the reactants was between 15 and 20. The other end of the capsule was then sealed and the samples heated at the desired temperature and pressure.

Polycrystalline samples were prepared by raising the temperature rapidly to 500°C while holding the pressure at 2 kb. The reaction was then allowed to proceed for 48 h under these conditions before being quenched. In order to grow single crystals, the degree of nucleation was controlled by bringing the temperature rapidly to 510–515°C then cooling at approximately 5°/h to 500°C before allowing the reaction to proceed for 6–14 days. After this treatment the pressure vessel was allowed to cool to room temperature.

Chemical Analysis

Samples of the cubic phase were decomposed in 2N hydrochloric acid to which a trace of nitric acid had been added. After the sample was completely dissolved, the solution was brought to pH 5 with 2N sodium hydroxide. The solutions were then diluted to 100 ml and the fluoride ion concentration was measured with an electrode† specifically sensitive to this ion.

The electrode was first calibrated against a series of standard solutions of known fluoride ion concentration. Since the activity coefficient is sensitive to the total ionic strength of the solution, care was taken to assure that this parameter had approximately the same value for the standard series as for the unknowns. The pH of the solutions was kept above 4 in order to avoid the formation of significant amounts of undissociated HF and HF_2^- both of which are not detected by the electrode. In addition, the pH had to be kept below 8 in order to eliminate interference by OH^-.

To satisfy these requirements the standard solutions were made up in the following manner. Samples of MoO_3 of approximately the same weight as the unknowns were dissolved in the same amount of 2N sodium hydroxide required to bring the unknown solution to pH 5. These solutions were then brought to pH 5 with 2N hydrochloric acid, and a known amount of a sodium fluoride stock solution was added. The solutions were then diluted to 100 ml. The potentials for these solutions were then measured and the results plotted against the log of the fluoride ion concentration. From the potential observed for an unknown it was then possible to determine the total fluoride present.

After the unknown solutions were analyzed for fluorine, they were passed through a silver reductor and the total molybdenum was determined by titration with ceric sulfate solution.

Samples of the orthorhombic phase, which was insoluble in various acids, were dissolved in 2N sodium hydroxide and then brought to pH 5 with 2N hydrochloric acid. The solutions were diluted to 100 ml and subjected to the same fluoride and molybdenum determinations.

The total reducing power of the products was confirmed by dissolving them in acid V^{5+} sulfate solution and titrating the resulting V^{4+} potentiometrically with ceric sulfate.

The results were: Calc. for $Mo_4O_{11.2}F_{0.8}$: Mo, 66.40; F, 2.37; Mo_{red} (as Mo^{5+}), 11.95. Found: Mo, 66.0; F, 2.4; Mo_{red}, 13.1. Calc. for $MoO_{2.4}F_{0.6}$: Mo, 65.82; F, 7.95; Mo_{red}, 40.16. Found: Mo, 65.5; F, 7.9; Mo_{red}, 42.8.

X-Ray Data

Cell parameters and X-ray diffraction powder intensity data were determined using a Norelco diffractometer with monochromatic radiation (AMR-202 focusing monochromator) and a high-intensity copper source [$\lambda(CuK\alpha_1) = 1.5405$ Å]. Cell parameters and space group were also determined by the single crystal precession technique using molybdenum radiation [$\lambda(MoK\alpha_1) = 0.70926$ Å].

Magnetic Measurements

A Faraday balance (*11*) was used to measure the susceptibility of powder samples of both materials over the temperature range 4.2–300°K.

Electrical Measurements

Resistance measurements were made on single crystals of the cubic material using the van der Pauw (*12*) technique. The samples used for these measurements were cubes 0.5–2.0 mm on an edge that had been ground to a thickness of about 0.2 mm. Four indium leads were attached to the crystals by means of ultrasonic soldering. The samples were then mounted on alumina plates and the leads attached

† Fluoride Ion Activity Electrode Model 94-09, Orion Research Inc., Cambridge, Mass.

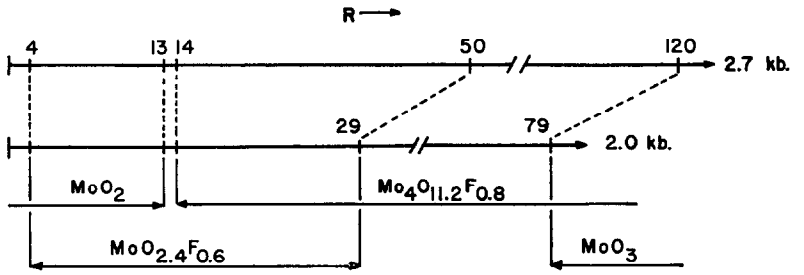

FIG. 1. Phase composition of the product versus the initial mole ratio (R) of MoO_3 : Mo in the reactants. In all cases hydrofluoric acid was present in excess.

to indium terminals. Gold paste leads may be substituted for the indium contacts.

The conventional four-probe configuration was used to measure the resistivity of the orthorhombic, $Mo_4O_{11.2}F_{0.8}$, phase.

Results

The mole ratios (R) of MoO_3 : Mo in the reaction mixtures were summarized in Fig. 1. The phase compositions of the products obtained when these mixtures of MoO_3 and Mo were fired at 500°C under 2-kb pressure for 48 h are shown.

Figure 1 can be subdivided as follows: For values of $R > 79$ unreacted MoO_3 is found in addition to a deep blue, almost black, phase which was orthorhombic and had the composition $Mo_4O_{11.2}F_{0.8}$. When $79 \geqslant R \geqslant 29$ only the orthorhombic phase was present in the product. If $29 > R > 14$ the product consisted of two phases, the orthorhombic phase and a cubic, gold-colored material of composition $MoO_{2.4}F_{0.6}$. The cubic phase was the only one detected in the product when $14 \geqslant R > 13$. For $13 \geqslant R > 4.5$ the product was the cubic phase and MoO_2, and when $R < 4$ only MoO_2 was formed.

Single crystals of $Mo_4O_{11.2}F_{0.8}$ were prepared in the form of flat needles up to 2 mm in length. Control of the degree of nucleation also resulted in cubes of $MoO_{2.4}F_{0.6}$ up to 2 mm on a side.

$Mo_4O_{11.2}F_{0.8}$

The powder pattern of this compound was similar to that observed for MoO_3 and was indexed on the basis of an orthorhombic cell, with $a = 3.878 \pm 0.005$, $b = 13.96 \pm 0.01$, and $c = 3.732 \pm 0.005$ Å. Single-crystal diffraction photographs revealed the systematic extinctions, $hkl: h + k = 2n + 1$ and $h0l: l = 2n + 1$ which are consistent with space groups Cmcm (No. 63), Ama2 (No. 40) and $Cmc2_1$ (No. 36). A detailed structure determination (*13*) showed the space group to be Cmcm. The structure was similar to that of the parent oxide MoO_3 (*14*)

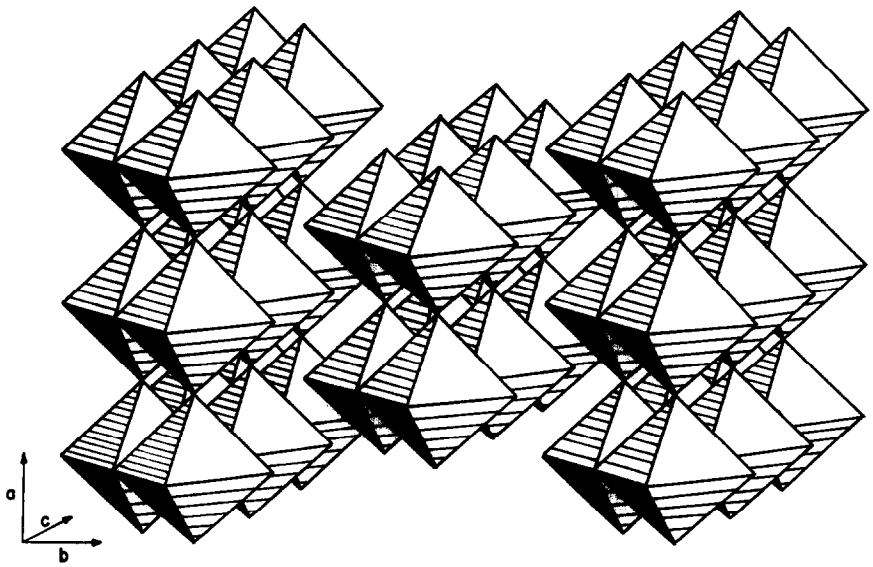

FIG. 2. The MoO_3 structure.

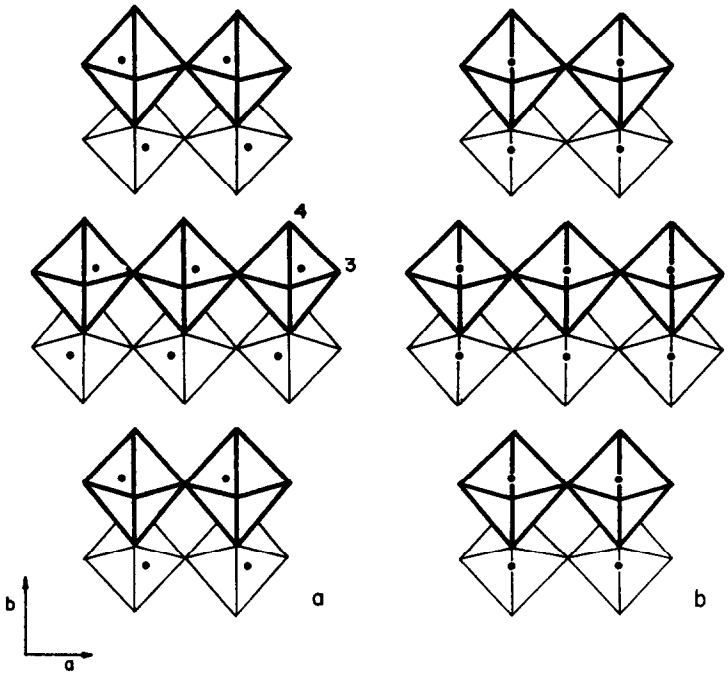

FIG. 3. Comparison of the structures of (a) MoO_3 and (b) $Mo_4O_{11.2}F_{0.8}$ illustrating the shift in the position of the molybdenum atoms (black dots) within the MoX_6 octahedra.

and isostructural with $Mo_4O_{10}(OH)_2$ (*6*). All three structures are composed of MoX_6 octahedra linked as shown in Fig. 2. The octahedra are joined by edges to form zigzag-shaped rows which are mutually connected by corners to form layers. The layers are placed side by side so that adjacent layers have no atoms in common. In this way three of the six anions surrounding each molybdenum atom are common to three MoX_6 octahedra and two of them are shared by two octahedra. The sixth anion is unshared and Wilhelmi (*6*) asserts, on the basis of observed bond lengths, that hydrogen bonds between pairs of these anions in adjacent layers account for the observed stoichiometry of $Mo_4O_{10}(OH)_2$.

Figure 3 is a plain view of the structure with the line of sight parallel to the *c* axis and illustrates the major difference between the structure of MoO_3 (Fig. 3a) and the structure of $Mo_4O_{10}(OH)_2$ and $Mo_4O_{11.2}F_{0.8}$ (Fig. 3b). Figure 4 illustrates the coordination of anions about the molybdenum atoms for MoO_3, $Mo_4O_{10}(OH)_2$, and $Mo_4O_{11.2}F_{0.8}$, respectively. Interatomic distances are presented for comparison in Table I.

Kihlborg (*5*) has shown that MoO_3 represents a

TABLE I

COMPARISON BETWEEN INTERATOMIC DISTANCES (IN Å) IN MoO_3 (*16*); $Mo_4O_{10}(OH)_2$ (*6*) AND THE CORRESPONDING DISTANCES IN $Mo_4O_{11.2}F_{0.8}$ (CF. FIG. 4)

Distance	MoO_3	$Mo_4O_{10}(OH)_2$	$Mo_4O_{11.2}F_{0.8}$
Mo–Mo across shared edge	3.438	3.427	3.462
Mo–Mo along [100]	3.963	3.888	3.878
Mo–Mo along [001]	3.696	3.734	3.732
Mo–O(2)	2.332	2.33	2.31
Mo–O(2′)	1.948	1.96	1.95
Mo–O(3)	1.734	1.96	1.96
Mo–O(3′)	2.251	1.96	1.96
Mo–O(4)	1.671	1.69	1.65

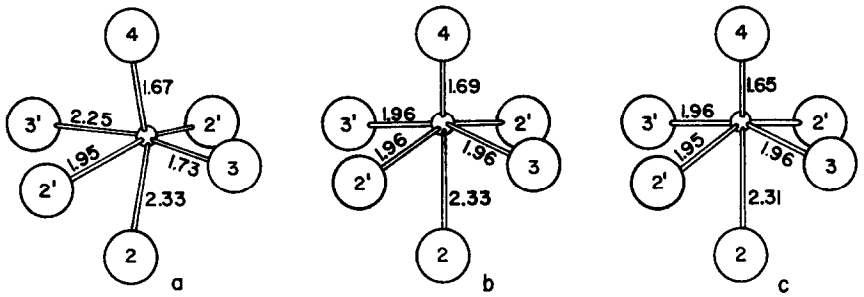

FIG. 4. The coordination of oxygen atoms (large spheres) around the molybdenum atoms (small spheres) in MoO_3 (a), $Mo_4O_{10}(OH)_2$ (b), and $Mo_4O_{11.2}F_{0.8}$ (c). (The numbering of atoms is in accordance with Refs. *5* and *6*).

transitional stage between octahedral and tetrahedral coordination with a strong tendency toward four-fold coordination. In the structure common to $Mo_4O_{10}(OH)_2$ and $Mo_4O_{11.2}F_{0.8}$ the tendency toward a more ideal octahedral configuration of anions around the molybdenum atoms is obvious. A shift toward octahedral coordination is also evident in the structure of $Mo_{18}O_{52}$, (*5*) which is composed of blocks with the $Mo_4O_{10}(OH)_2$ structure joined by a complicated shear mechanism.

Wilhelmi (*6*) noted that a shift toward octahedral coordination should result in an increase in the thickness of a layer, and hence in the spacing between layer centers. Such an effect is observed if one compares the distance between layers in MoO_3 (6.93 Å) to that in $Mo_{18}O_{52}$ (7.23 Å). He also demonstrates that this effect is much less pronounced in $Mo_4O_{10}(OH)_2$ (7.04 Å) because of hydrogen bonding between adjacent layers. In $Mo_4O_{11.2}F_{0.8}$ the interlayer spacing, 6.98 Å, is less than that of either $Mo_4O_{10}(OH)_2$ or $Mo_{18}O_{52}$; in $Mo_4O_{11.2}F_{0.8}$ the distance between "unshared" anions in adjacent layers, 2.81 Å, compares favorably with that observed in $Mo_4O_{10}(OH)_2$, 2.80 Å, where these anions are presumably hydrogen bonded.

$MoO_{2.4}F_{0.6}$

At reaction temperatures of 475–525°C a single phase of this composition is formed when R is held near 14. Outside of this temperature range MoO_2 is found in the product.

Single-crystal diffraction photographs indicate the compound to be cubic with Laue symmetry m3m and no systematic extinctions. The space group Pm3m was assumed for this material. The cell parameter was found to be $a = 3.842 \pm 0.005$ Å. The pycnometrically determined density was $d_m = 4.1 \pm 0.1$ g/cm^3 and the calculated density was $d_c = 4.27$ g/cm^3, indicating a cell containing one formula unit.

A trial structure was assumed similar to that of ReO_3 (*15*) with oxygen and fluorine atoms distributed randomly in the positions $(\frac{1}{2},0,0)$; $(0,\frac{1}{2},0)$; $(0,0,\frac{1}{2})$ and molybdenum atoms at positions $(0,0,0)$. Parthé's (*16*) intensity program was used to calculate intensities based on the trial structure. The occupancy factors for oxygen and fluorine were adjusted to comply with the observed stoichiometry. The temperature factor was set at 1.00 based on temperature factors observed for other molybdenum oxides. The resulting intensities gave a reliability index:

$$R = \frac{\sum |I_0 - I_c|}{\sum |I_0|} = 0.12$$

Discussion

Single crystals of $MoO_{2.4}F_{0.6}$ were prepared by holding the reactants at 500°C under 2-kb pressure for 6 days and then quenching the pressure vessel in cold water. Activation energies were calculated from the resistivity data and ranged from 0.02–0.06 eV. Photomicrographs of the surfaces of these crystals showed dislocations and growth steps as well as many small cracks. Crystals were also obtained by repeating the crystal runs, but terminating the reaction by slow cooling the pressure vessel at 100°C/h. Microscopic examination revealed no cracks in these crystals, and the apparent activation energy was lowered to 0.006 eV. Crystals grown at 500°C and 2-kb pressure for 10 days before slow cooling showed activation energies of 0.003 ± 0.001 eV. The apparent activation energy appears to be caused by crystal imperfections that can be partially annealed out by holding the sample under growth conditions for extended periods of time.

The resistivity curve shown in Fig. 5 is that of a specimen held under growth conditions for 14 days before slow cooling. The resistivity approaches 10^{-2} Ω cm, even at 4.2°K (point not shown), suggesting that the compound is metallic.

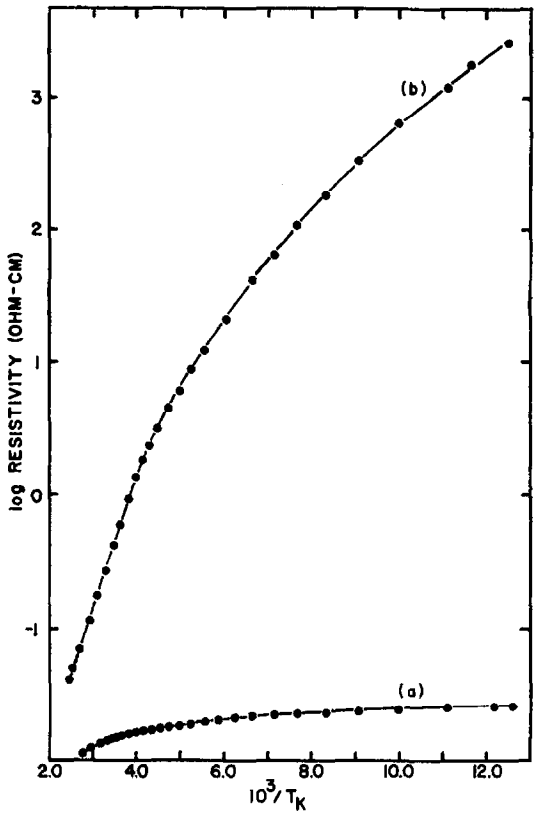

FIG. 5. Resistivity vs $10^3/T_k$ for $MoO_{2.4}F_{0.6}$ (a) and parallel to the c axis in $Mo_4O_{11.2}F_{0.8}$ (b).

The resistivity profile for $Mo_4O_{11.2}F_{0.8}$ shown in Fig. 5 was obtained from measurements made in the direction parallel to the long dimension of the needle-like crystals, which corresponds to the crystallographic c axis. The shape of the crystals was such that it was not possible to attach leads for measurement along any other axis. The behavior observed is that of a semiconductor with a low-temperature activation energy of 0.2 eV.

The electrical properties of these materials can be related to differences between their structures. For the ReO_3 structure, in which the octahedra are regular and share corners in three dimensions, the conditions are optimized for the formation of collective-electron π^* orbitals of the type suggested by Goodenough (*10*). However, in MoO_3-related structures corner sharing occurs only along the a axis. This is consistent with the observation that $MoO_{2.4}F_{0.6}$ is metallic whereas in $Mo_4O_{11.2}F_{0.8}$ conductivity parallel to the c axis requires an activation energy. It can also be seen from Table II that the properties of the oxyfluorides are consistent with the prediction of Magnéli (*7*), namely that as the

TABLE II

FORMAL OXIDATION STATE AND COORDINATION NUMBER OF MOLYBDENUM IN COMPOUNDS WITH STOICHIOMETRIES APPROACHING MoX_3

Compound	Oxidation state	Coordination No.
MoO_3	6.00	4
$Mo_4O_{11.2}F_{0.8}$	5.80	5
$Mo_{18}O_{52}$	5.78	5
Mo_4O_{11}	5.50	6
$MoO_{2.4}F_{0.6}$	5.40	6

amount of reduced molybdenum in the compound increases, the coordination number of molybdenum approaches a maximum. From Table II it can be seen that for the oxyfluoride $MoO_{2.4}F_{0.6}$ the coordination number of molybdenum is six.

The magnetic susceptibility of both materials was measured over the temperature range 4.2–300°K. In both cases a marked increase in susceptibility was observed as the temperature approached that of liquid helium. However, for all samples measured a plot of $1/X_M$ vs T proved to be linear over the range 4.2–140°K. The intercept of these curves was at the origin and above 140°K the magnitude of the susceptibility was about 0.05×10^{-6} emu/g. In the upper half of the 4.2–300°K range small errors in the measurement caused a great deal of scatter among the calculated values of $1/X_M$.

Values of the Curie constant calculated from the slope of the $1/X_M$ vs T plots varied over the range $1.0–1.5 \times 10^{-3}$ emu °K/mole. If this temperature-dependent contribution is subtracted, under the assumption that it represents a magnetic impurity, then $MoO_{2.4}F_{0.6}$ shows a temperature-independent susceptibility of 0.01×10^{-6} emu/g, which is consistent with metallic behavior. The similarly corrected, temperature-independent susceptibility of $Mo_4O_{11.2}F_{0.8}$ was -0.02×10^{-6} emu/g.

A study was also made of the effect of elevated reaction pressures on the phase composition of the products. At 2.7 kb a shift to higher values of R was observed for both boundaries of the orthorhombic phase, as shown in Fig. 1. No shift was observed for any of the other phase boundaries.

Acknowledgment

The authors wish to thank Dr. John B. Goodenough for his comments and suggestions. In addition, we would like to thank Dr. Marc Richman for his assistance with the microscopic studies.

Addenda

In a recent publication, A. Sleight, *Inorg. Chem.* **8**, 1764 (1969) has independently reported the semiconducting compound $Mo_4O_{11}F$ as well as cubic products with the composition $MoO_{3-\delta}F_\delta$ (where $0.74 \leqslant \delta \leqslant 0.97$). The differences reported by Sleight concerning the characteristics and range of homogeneity of the cubic phase are undoubtedly due to differences in the experimental conditions reported for the preparation of the samples.

References

1. G. HÄGG AND A. MAGNÉLI, *Rev. Pure Appl. Chem.* **4**, 236 (1954).
2. L. KIHLBORG, *Arkiv Kémi* **21**, 471 (1963).
3. A. MAGNÉLI, *Acta Chem. Scand.* **2**, 501 (1948).
4. Ref. 3, p. 861.
5. Ref. 2, p. 443.
6. K. A. WILHELMI, *Acta Chem. Scand.* **23**, 419 (1969).
7. A. MAGNÉLI, *J. Inorg. Nucl. Chem.* **2**, 330 (1956).
8. D. E. LA VALLE, R. M. STEELE, M. K. WILKINSON, AND H. C. YAKEL, JR., *J. Amer. Chem. Soc.* **82**, 2433 (1960).
9. A. FERRETTI, D. B. ROGERS, AND J. B. GOODENOUGH, *J. Phys. Chem. Solids* **26**, 2007 (1965).
10. J. B. GOODENOUGH, *Bull. Chim. Soc. France* **4**, 1200 (1965).
11. B. L. MORRIS AND A. WOLD, *Rev. Sci. Instru.* **30**, 1937 (1968).
12. L. J. VAN DER PAUW, *Philips Res. Repts.* **16**, 187 (1961).
13. J. W. PIERCE, M. VLASSE, AND A. WOLD. To be published.
14. Ref. 2, p. 357.
15. K. MEISEL, *Z. Anorg. Allgem. Chemie* **207**, 121 (1932).
16. W. JEITSCHKO AND E. PARTHÉ, "A Fortran IV Program for the Intensity Calculation of Powder Patterns," University of Pennsylvania Press.